iJRASET
International Journal For Research in Applied Science and Engineering Technology

INTERNATIONAL JOURNAL FOR RESEARCH

IN APPLIED SCIENCE & ENGINEERING TECHNOLOGY

Volume: 11 **Issue:** III **Month of publication:** March 2023

DOI: https://doi.org/10.22214/ijraset.2023.49447

www.ijraset.com

Call: 08813907089 | E-mail ID: ijraset@gmail.com

International Journal for Research in Applied Science & Engineering Technology (IJRASET)
ISSN: 2321-9653; IC Value: 45.98; SJ Impact Factor: 7.538
Volume 11 Issue III Mar 2023- Available at www.ijraset.com

Bidirectional Power Control Strategy for Super Capacitor Energy Storage System based on MMC DC-DC Converter

Swetha. M[1], G. Swarna Latha[2], D. Swathi[3], N. Upendra Reddy[4], N. Varun Kumar Reddy[5]
[1, 2, 3, 4, 5]*Annamacharya Institute of Technology and Sciences, Rajampet*

Abstract: ***In order to equip more high-energy pulse loads and improve power supply reliability, the vessel integrated power system shows an increasing demand for high-voltage and large-capacity energy storage systems. Based on this background, this paper focuses on a super capacitor energy storage system based on a DC-DC converter. This paper analyzes the different topology of Hybrid Energy Storage System (HESS) and Demand Management System using HESS. Taking into account the shortcomings of the traditional bidirectional power control strategy, this paper proposes a control strategy where the HESS module of each branch independently controls the voltage of the sub-module capacitor. The outputs are validated and verified using MATLAB Simulink platform.***

I. INTRODUCTION

The integrated power system has received extensive attention in the DC power distribution. In the future, it will be one of the inevitable technical routes for renewable energy systems [1][3]. In recent years, with the increasing demand for higher power supply reliability, and equipment of pulsed loads and new high-energy weapons, energy storage systems have become an indispensable part of the second-generation [4], [5]. Therefore, the energy storage converter connected to the medium voltage DC (MVDC) grid needs to be characterized by high voltage and large capacity, voltage conversion, electrical isolation and bidirectional conversion. It is widely used in high-voltage and large-power applications because of its modular structure and fault tolerance [6]. For high-voltage rail transit vehicles, the control strategies of super capacitor energy storage system based on Modular Multilevel Converter (MMC) are studied in [7], [8]. These two papers realize the balanced decoupling control of the power of super capacitors, and put forward the corresponding energy management strategies. In [9], the control strategy of modular multilevel energy storage system under two operating conditions of grid voltage symmetry and asymmetry is studied, which solves the problem of charge state balance of energy storage elements. To realize the electrical isolation and voltage conversion, isolated bidirectional DC-DC converter needs to be used between MVDC grid and LVDC grid. It is a bidirectional DC-DC converter with electrical isolation capability and modular symmetrical structure. It has attracted extensive attention in the fields of electric vehicles, DC micro grids and energy storage systems However, the above literatures study the application scenario of connecting resistive load on the LVDC bus of MMC-DAB. Their control strategy is that MMC controls the voltage of sub-module capacitors and converter controls the voltage of the LVDC bus. If this strategy is extended to the application scenario with energy storage unit connected on the LVDC side, the converter module usually controls the port current of the energy storage unit. To better control the port current of the energy storage unit, the filter inductor needs to be connected between the converter and the energy storage unit. However, this will increase the volume and weight of the device, and the stability margin of converter control system is small. Especially when discharging the super capacitor, the filter inductor and the filter capacitor at the later stage of converter control form an LC filter with large output impedance, which is easy to cause stability problems [10].

II. HYBRID ENERGY STORAGE SYSTEMS

A. Battery Modelling

The battery was a source element, and its equivalent circuit model implemented in the EMR element is calculated by:

$$u_{cell} = u_{cell\_OC}(SOC_{cell}) - r_{cell} i_{cell}$$

$$SOC_{cell} = SOC_{cell\_init} - \frac{1}{C_{cap}} \int_0^t i_{cell}$$

$$C_{cap} = 3600 Q_{bat}$$

Where r_{cell} is the equivalent resistance of a cell module and $Q_{bat}$is the cell storage capacity. The open-circuit voltage of a cell module $U_{cell\_OC.}$ is a function of its state-of-charge. It was demonstrated by a look-up table in this work. The SOC of the cell module was determined by the Coulomb counting method. Because of the parallel and series connection of the cell modules, the total voltages and currents of the battery are given by the equations below.

$$u_{bat} = u_{cell} n_{se\_bat}$$
$$i_{bat} = i_{cell} n_{pa\_bat}$$

Where n_{se} and n_{pa} are the number of modules connected in series and the number of parallel branches of the serial ones, respectively.

B. Super Capacitor Modelling

The super capacitor was also a source element, which is represented as a green oval. The SC mathematical model is shown in the following equation.

$$u_{sc\_mod} = u_{sc\_0} - r_{sc\_mod} i_{sc\_mod} - \frac{1}{C_{mod}} \int_0^t i_{sc\_mod} dt$$

Where r_{sc} is the internal resistance and *C* is the capacitance.

C. Bidirectional DC/DC Converter Modeling

The bidirectional DC/DC converter boosted the SC voltage equal to that of the battery in the semi-active configuration. The SC can both provide and receive energy with that converter. The converter, consisting of an inductor and two power electronic switches. The inductor was an accumulation element that has the dynamic model below:

$$i_{sc} = \frac{1}{Ls + r}(u_{sc} - u_{ch})$$

D. Design of Modular Multilevel Inverter

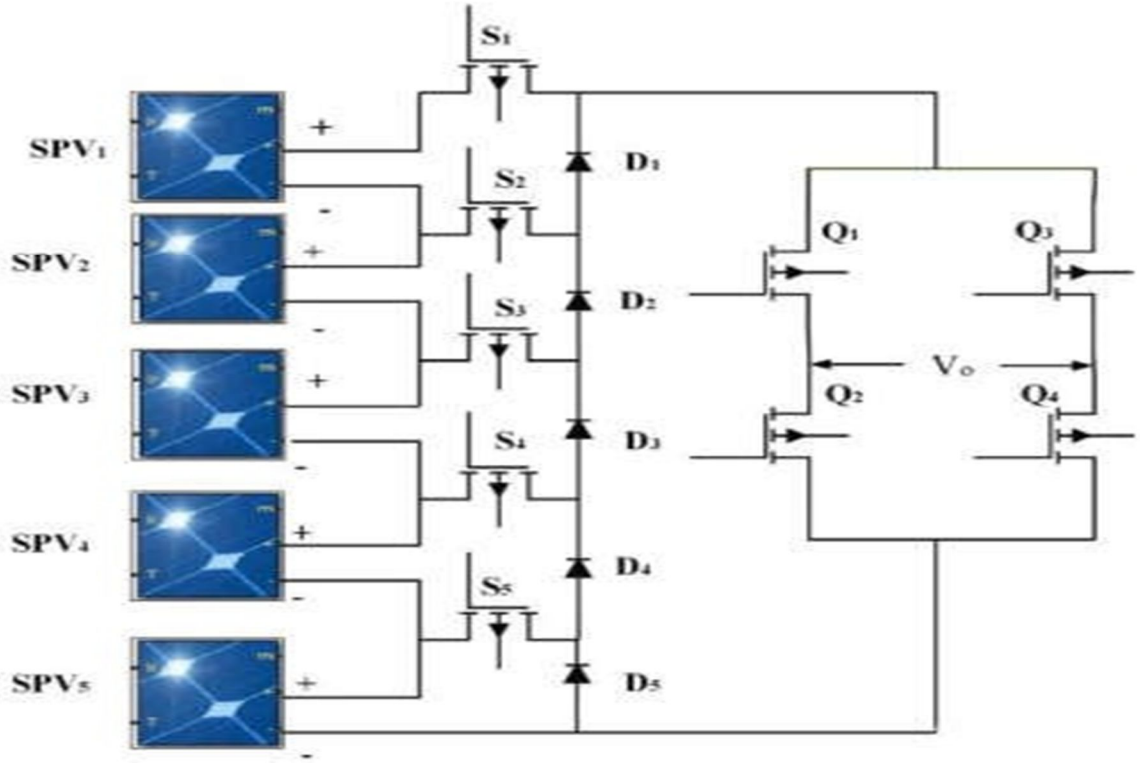

Figure.1(a) 11-Level MMI.

ISSN: 2321-9653; IC Value: 45.98; SJ Impact Factor: 7.538
Volume 11 Issue III Mar 2023- Available at www.ijraset.com

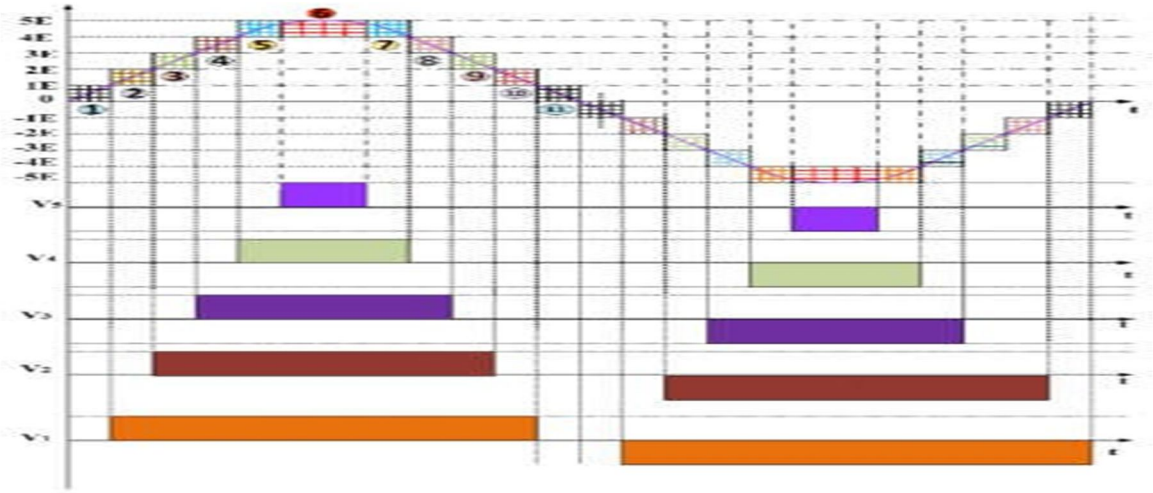

Figure.1(a) Pulse width modulation for MMI.

The proposed MLI topology involves a combination of two topologies including a level generation unit of the inverter (basic entity) and full bridge inverter. The basic entities connected in a cascaded fashion to generate staircase voltage levels only in positive polarity (includes zero levels) on voltage magnitude of the input DC sources either symmetric or asymmetric. Unidirectional switches are used in this topology which operates at high switching frequency as shown in Fig. 1 (a) & (b).

The DC voltage sources are making it suitable to be utilized for energy storage system and solar PV applications because of the isolated voltage sources. The voltage magnitude of DC sources are the same. Hence the presented topology acts in the symmetric condition. The generation of voltage level varies in symmetric and asymmetric condition. Changing the polarity of the generated voltage level for every half cycle is essential to operate as an inverter. So, the full bridge inverter is connected in series with a cascaded fashion of basic entity which can produce zero, positive and negative voltage levels. This full bridge inverter does not require bidirectional switches and it operates in fundamental switching frequency. Both high and fundamental switching frequencies are utilized in the proposed topology to generate the desired output voltage levels.

The total number of switches are equal to the total number of driver circuits in the topology as it utilizes only unidirectional switches. The proposed configurations operate at both symmetric and asymmetric conditions without changing the structure of MLI. The MMI is a convenient solution for PV applications.

The MMI topology has the combination of "2S+1" level generation and polarity generation. The input voltage divider is composed of five series solar PV modules labeled as SPV1, SPV2, SPV3, SPV4, and SPV5. The divided voltage is transmitted to the circuit consisting of controlled and uncontrolled devices marked as S1, S2, S3, S4, S5, D1, D2, D3, D4, and D5 which is then combined as one H-bridge (Q1, Q2, Q3, and Q4).

The total number of switches (K), S is denotes as number of switches without a full bridge inverter. The below equations describe the number of sources and switches required for the proposed methodology.

Total number of switches,

K= S + 4 for S = 5, K = 5+4 = 9 switches

Number of levels

N_{Level} = 2S + 1 for S = 5, N_{Level} = 2(5) + 1= 11

Number of levels

N_{Level} = K+2 for K = 9, N_{Level} = 11Levels

The proposed MMI topology is a suitable solution for RES applications. In general, multiple PV panels associated with numerous boost converters are obligatory for gaining the required MMI output.

1) Mode of Operations

The RES fed DC-DC converter regulates the voltage applied to the MLI. It has solar PV module whose terminal voltage must be equal to the reliable Power. The power produced from the given PV module fundamentally depends on solar irradiance (1000W/m2) and temperature (25ºC). Moreover, the terminal voltage of the RES and PV module must be equal to the resultant.

The major enhancement of this topology is the availability to replace the faulty unit easily in case of fault manifestation in any of the switches of MLI, which would offer an uninterrupted power supply with a reduction in the required voltage level. In this, five separate DC supply and boost converters are associated to the MMI.

This proposed topology generates 11-level output voltage with the help of 9 switches and 5 sources. The voltage level generation based on the switching table. Moreover, the H-bridge circuit topology is utilized as a part of the development and implementation of the symmetric and asymmetric. The several voltage levels of the MLI are attained as follows:

(+) ^{VE} half cycle:+1/5 Vdc,+2/5 Vdc, +3/5 Vdc,
+4/5 Vdc, +Vdc

(-) ^{VE} half cycle: -1/5 Vdc, -2/5Vdc,-3/5 Vdc,
-4/5 Vdc, -Vdc

a) generate (stage-I), voltage levels of Vo = +1/5Vdc, S5 is turned ON at the positive half cycle. By utilizing the proper switching sequence of S5, Q1, and Q4 are turned on and the voltage applied to the load terminals is +1/5Vdc. Mode - 1 is designed based on the switching sequence of SPV5+-D4-D3-D2- D1-Q1-RL+-Q4-SPV5-.

b) The generate (stage-II), voltage levels of Vo = +2/5Vdc, S4 are turned ON at the positive half cycle. By utilizing the proper switching sequence S4, Q1, and Q4 are turned ON and the voltage applied to the load terminals is +2/5 Vdc. Mode - 2 is designed based on the switching sequence of SPV4+-D3-D2- D1-Q1-RL+-Q4-SPV4-.In stage II, solar PV voltage of (SPV4 +SPV5) is added to develop the next positive level output voltage of +2/5Vdc.

c) To generate (stage-III), voltage level of Vo = +3/5Vdc, S3 is turned ON at the positive half cycle. By utilizing the proper switching sequence S3, Q1, and Q4 are turned ON and the voltage applied to the load terminals is +3/5Vdc. Mode - 3 is designed based on the switching sequence of SPV2+-D1-Q1-RL+- Q4-SPV2- which shows the current path as illustrated in Figure 1.3 (c). In stage-III, also solar PV voltage of (SPV3 +SPV4 +SPV5) is added to develop the next positive level output voltage of +3/5Vdc.

d) To generate (stage-IV), voltage level of Vo = +4/5Vdc, S2 is turned ON at the positive half cycle. By utilizing the proper switching sequence S4, Q1, and Q4 are turned ON and the voltage applied to the load terminals is +4/5Vdc. Mode - 4 is designed based on the switching sequence of SPV2+-D1-Q1-RL+- Q4-SPV2- . In stage- IV, includes solar PV voltage of (SPV2+SPV3 +SPV4 +SPV5) to develop the next positive level output voltage of +4/5Vdc.

e) To generate (stage-V), voltage level of Vo = +Vdc, S1 is turned ON at the positive half cycle. Using the proper switching sequence S1, Q1, and Q4 are turned ON and the voltage applied to the load terminals is +Vdc. Mode - 5 is designed based on the switching sequence of SPV1+-Q1-RL+-Q4-SPV1- which shows the current. In stage -V, solar PV voltage of (SPV1+SPV2+SPV3 +SPV4 +SPV5) is added to develop the next positive level output voltage of +Vdc.

f) To generate (stage-VI), voltage level of Vo = 0, all the switches are turned OFF at the positive half cycle. Using the proper switching sequence Q1 and Q4 are turned ON and the voltage applied to the load terminals is 0. In Mode - 6 is designed based on the switching sequence of Q1-RL+-Q4.

g) To generate a negative switching device of an MMI which is proportional to the number of voltage level of -Vo= -1/5Vdc,-2/5Vdc,-3/5Vdc,-4/5Vdc,-Vdc, similar switching combination is used at the negative half cycle for the modes of operation (7-11). The proper switching sequence to turn ON and OFF the power electronic devices and RES to deliver 11 level output voltage.

2) PWM Techniques for MMI

This present research focuses on multicarrier PWM for eleven level inverter. The switching angle of the PWM pulses determines by the multicarrier PWM method. This includes the multiple carrier techniques such as APOD, PD and POD along with sinusoidal techniques. The modified level shift carrier is mainly focused on the correlation between two low recurrence balancing signals with a triangular high recurrence bearer. Figure 2, shows the proposed modular multilevel inverter with gating PWM generation.

ISSN: 2321-9653; IC Value: 45.98; SJ Impact Factor: 7.538
Volume 11 Issue III Mar 2023- Available at www.ijraset.com

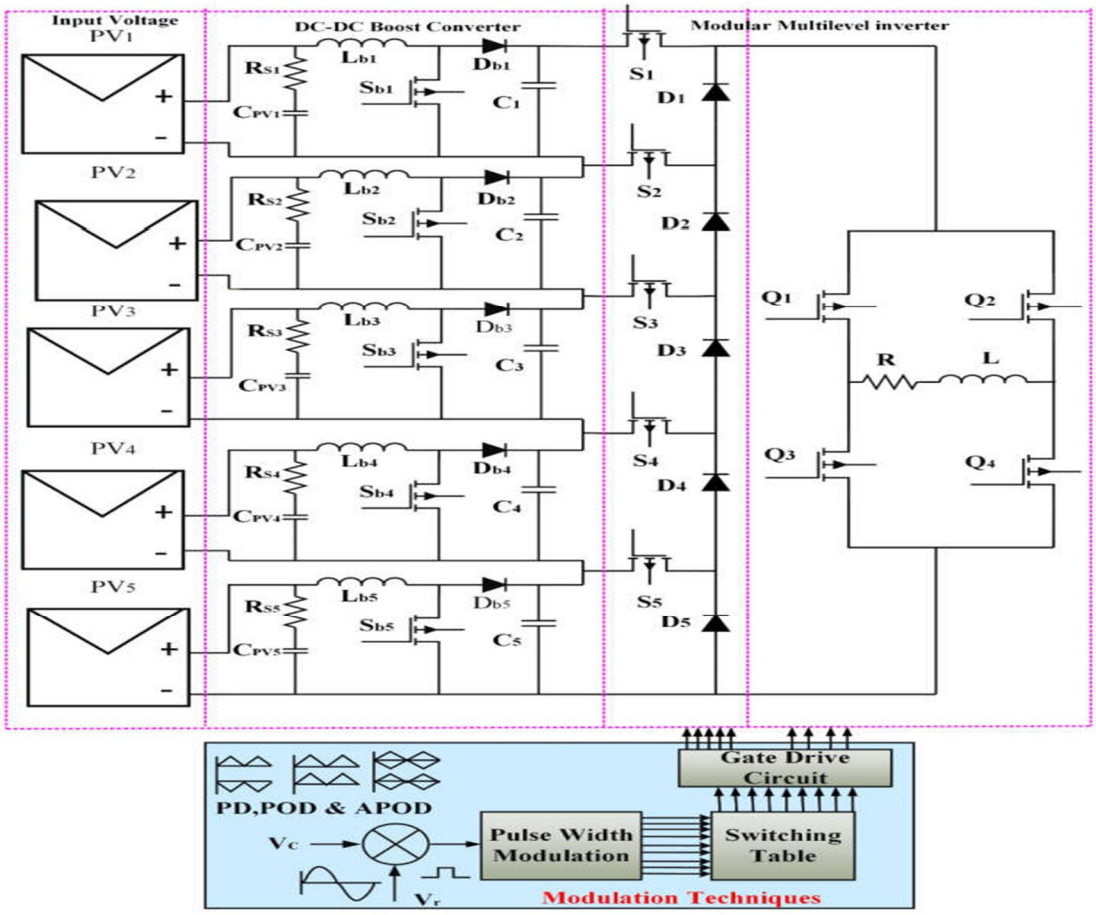

Figure 2. Proposed modular multilevel Inverter with Gating PWM

3) Design of DC-DC converter

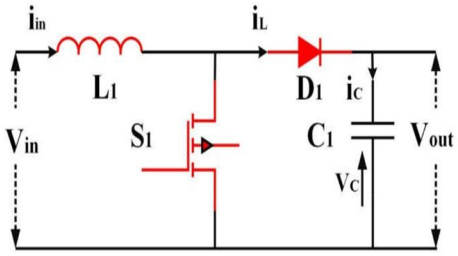

Figure 3. Boost converter

DC-DC converter plays an important role in PV installations because the PV generated voltage is not sufficient to meet the load requirement. In this process, the boost converter produces maximum power through the input of the proposed MLI as shown in Figure 2. The boost converter is also called a step-up converter because the name of the converter indicates a step-up DC voltage input and a DC voltage output. The boost converter comprises an inductor, diode, IGBT switch and capacitor. The capacitor is designed to eliminate the ripples in the output voltage. The boost converter has two different operating conditions in continuous conduction mode.

If the converter works in continuous conduction mode as shown in Fig.3, the inductor current will never fall to the same rating of five DC-DC converters are designed for the proposed system with the same number of duty cycle. The two critical parameters of the DC-DC converter are inductor and capacitor which are designed to get the output voltage of 24 V. The ripple value of inductor. Current and fs is the switching frequency of the converter.

where Iout (max) is the maximum current from the PV module under maximum irradiance conditions (i.e. at 1 kW/m2).The value of the capacitor is determined by using equations, where is the ripple value of capacitor current and fs is the switching frequency converter

$$C_1 = \frac{I_{out*D}}{f_{s*\Delta V_{out}}}$$

$$\Delta V_c = (2\%\ to 4\%) * \Delta V_{out} * \frac{I_{out}}{I_{in}}$$

$$\Delta V_c = 0.03 * 24 * \frac{5}{10} = 0.36$$

Substitute the $\Delta V_c, D$ then,

$$C_1 = \frac{5 * 0.67}{3 * 10^3 * 0.36} = 300\mu F$$

III. SIMULATION

A. Energy Management Strategies

The Figure.4 Shows the Simulation Model. The energy-based strategy relates to the squared SC voltage because the SC energy is proportional to it. The SOC-based strategy was defined by the relationship between the current measured SC voltage and the minimum SC voltage value Usc-min, which was also used to calculate the SOC percentage of the SC in this study.

Fig.4 illustrates the Simulation Model of MLI with ESS. If the battery SOC is a nonlinear function with the battery voltage, then the SC SOC is defined to be linear with the voltage of the SC. This has special effects on the HESS. Finally, the voltage-based algorithm coefficient is the square of the SOC-based strategy. Although all approaches are computed in terms of SC voltage values, each strategy shows the variation of the SC's ability with different proportions.

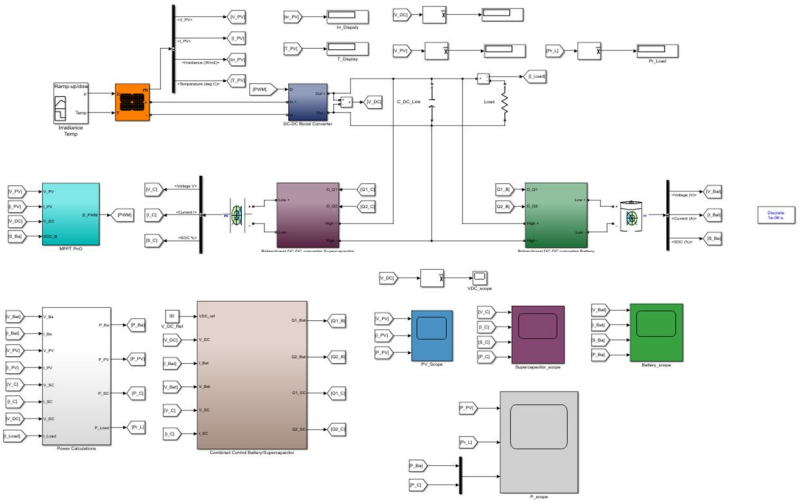

Figure 4. Simulation Model of MLI with ESS.

Besides, an SC charging control block, shown in Figure 5, was combined with the mentioned strategies to help the SC recover energy in the absence of vehicle power demand. The SC would be charged with a preset current if the absolute value of the traction current was less than e. In the simulation, the value of ε was 0.05 A. That was a very small value to avoid chattering.

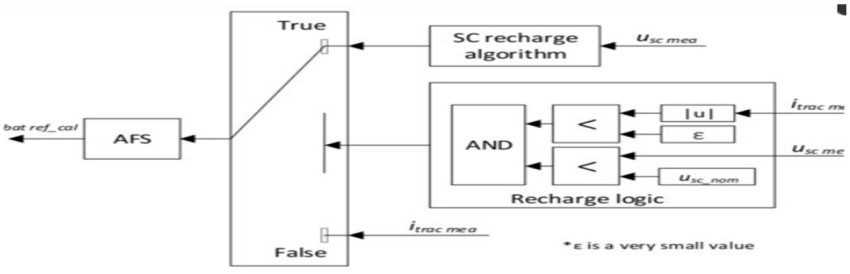

Figure 5. Super capacitor recharge control block.

IV. SIMULATION RESULTS

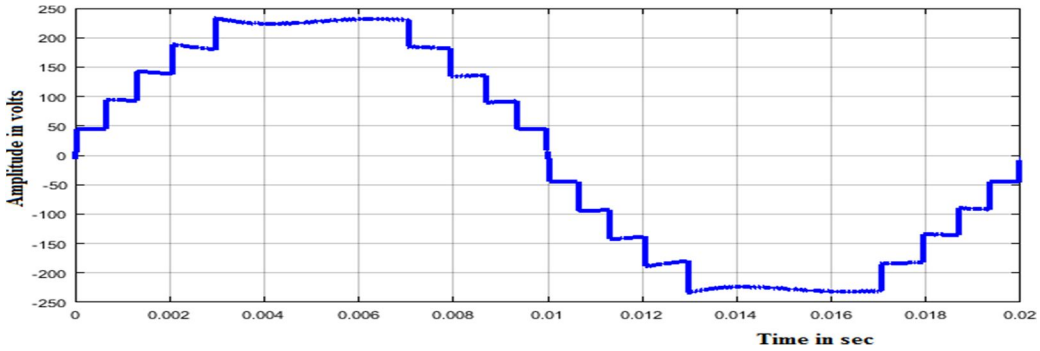

Figure, 6.Eleven level output of MMI

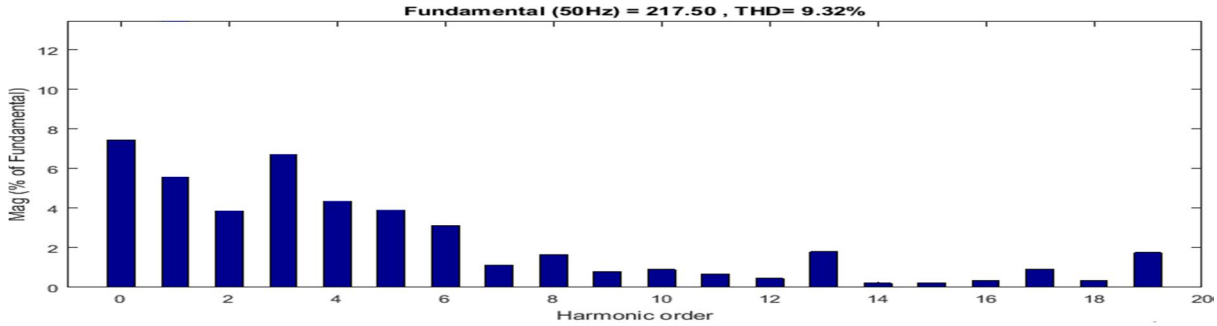

Figure 7. Voltage THD for RL load

In the proposed model, each input variable of switching angle and modulation index obtained from Controller and evaluate the output data. The fig.6 shows the output of 11-level inverter voltage. The next process is fine tuning the optimum output variables of eleven level output voltage with least THD and for minimizing the error speed as shown in Figure 7. The simulation result shows the verification of input and output data pairs to obtain the optimized THD. The obtained optimally selected data are trained.

A. PV Outputs

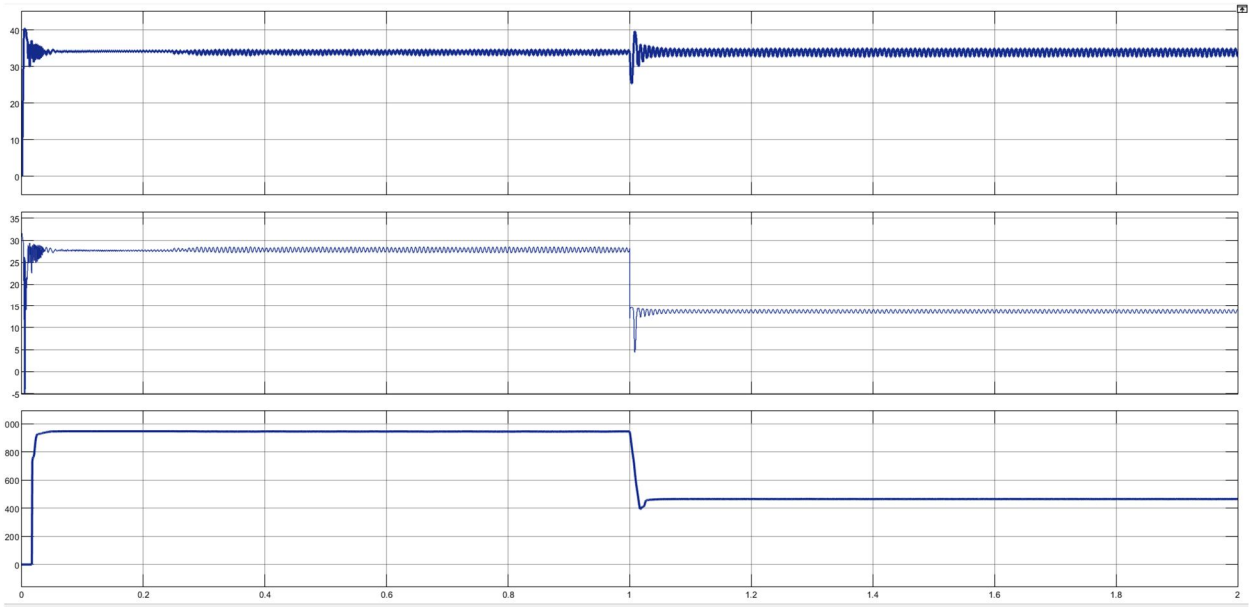

Figure 8. PV Outputs voltage and current.

B. Battery Outputs

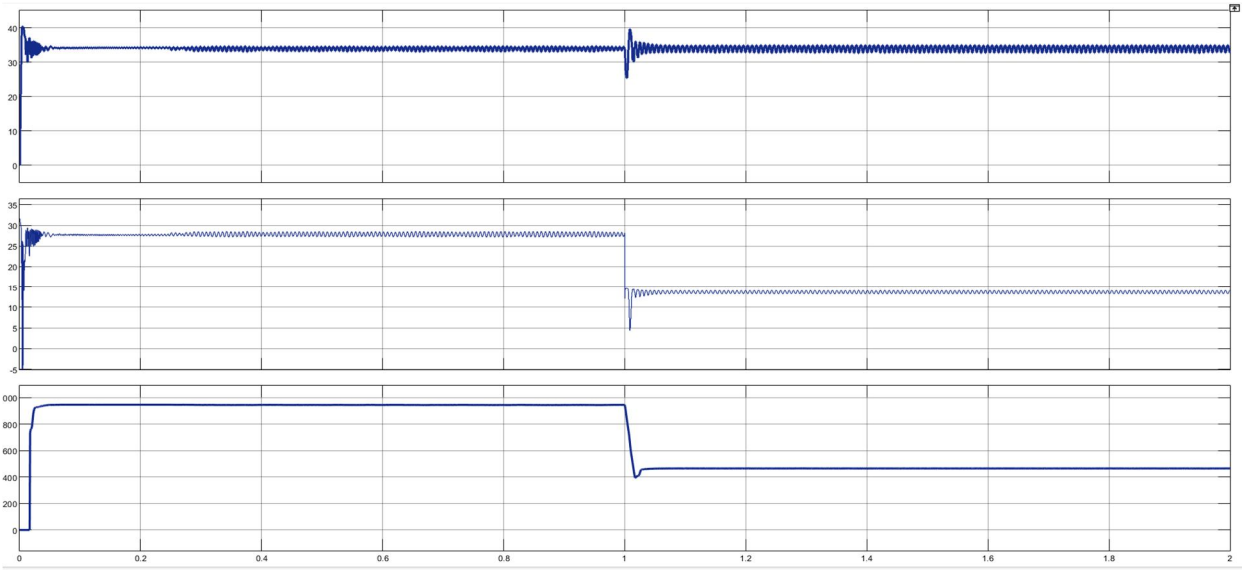

Figure 9. Battery Outputs voltage and current.

C. Super Capacitor Outputs

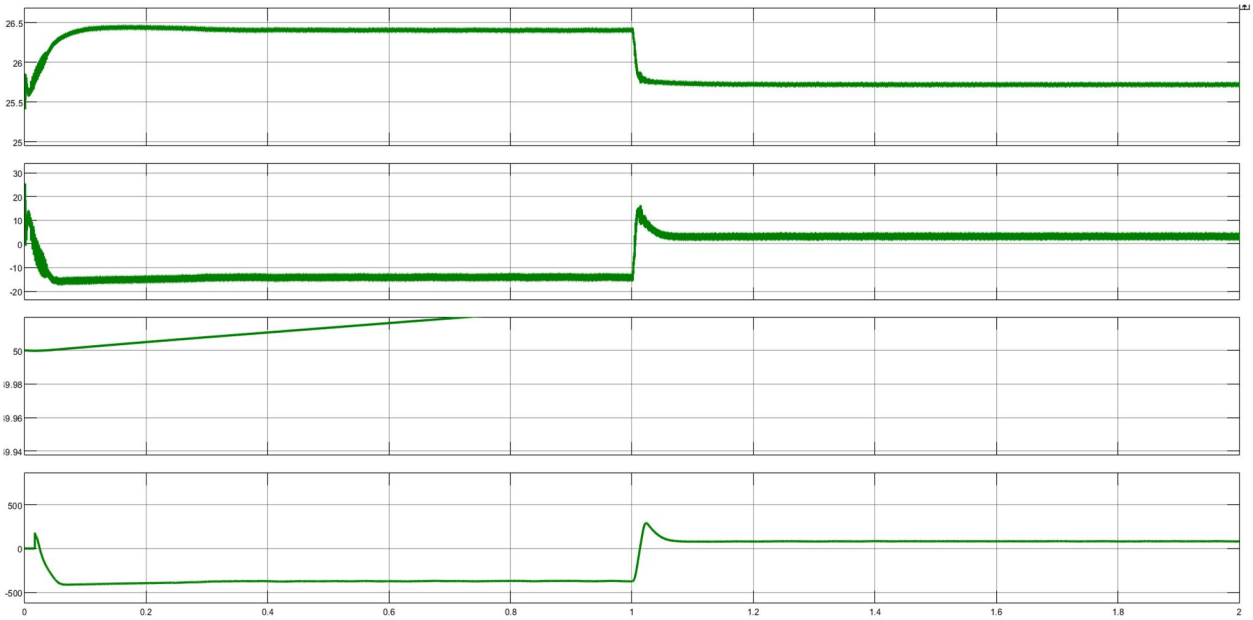

Figure 10. Super Capacitor Outputs voltage and current.

The Figure 8,9, and10 shows the PV outputs, Battery Outputs and Super Capacitor Outputs. To sum up, the energy-based strategy had the greatest effects on urban cycles whose driving conditions varied considerably and consecutively. The SOC-based and voltage-based strategies were more effective than the energy-based one when operated under driving conditions with less fluctuation. Because of the significant reduction of the battery rms current and peak current, the battery voltage drop was also minimized. Thus, undesirable effects on the electric drive system were avoided thanks to the semi-active HESS configuration and the EMS. It could consequently be seen that the battery/SC dual-source system and the proposed filtering strategies were more worthy for electric cars than for other kinds of EVs that work under smoother driving conditions. The impact of the proposed strategies on the SC under several initial conditions such as the SC being fully charged before the vehicle operating or the car not having been used for a long time needs to be illustrated. Hence, simulation were carried out at four initial voltages of the SC including U, 0.75U, 0.5U, and 0.25U.

V. CONCLUSION

This paper proposed three simple, but effective filter-based strategies for the power allocation of a battery/SC EV, which relied on the SC stored energy, SOC, and voltage. We aimed to show the feasibility in a real-world implementation. Furthermore, the system control and EMS can be transferred from the simulation development. These proposed methods were compared to each other before they were analyzed together with a pure battery car and a conventional filtering method under the same working conditions to find the most effective solution. Simulation results showed that the HESS and EMS had significant roles in protecting the battery under fluctuating driving conditions. In the super capacitor of the battery of the HESS with the energy-based strategy was only about one-third of that of the battery-only vehicle. The super capacitor energy storage unit is connected to LVDC bus, which is conducive to enhance the flexibility and reliability of the energy regulation of the DC grid, and also provides power source for pulse loads on board.

REFERENCES

[1] W. Ma, ``On comprehensive development of electrization and information-zation in naval ships," J. Nav. Univ. Eng., vol. 22, no. 5, pp. 14, Oct. 2010.
[2] M. Weiming, ``Development of vessel integrated power system," in Proc. Int. Conf. Electr. Mach. Syst., Beijing, China, Aug. 2011, pp. 112.
[3] W. Ma, ``Development of vessel integrated power system," Ordnance Knowl., vol. 4, no. 3, pp. 3133, 2011.
[4] L. Fu, L. Liu, G. Wang, F. Ma, Z. Ye, F. Ji, and L. Liu, ``The research progress of the medium voltage DC integrated power system in China," Chin. J. Ship Res., vol. 11, no. 1, pp. 7299, Feb. 2016.
[5] S. Wan and Z. Meng, ``Current status and prospects of analysis technologies of shipboard integrated power system," Chin. J. Ship Res., vol. 14, no. 2, pp. 107117, Apr. 2019.
[6] H. Zhang, W. Shao, X. Wei, and N. Li, ``Study on fault tolerant control strategy for sub-modules of modular multilevel converter," in Proc.Asia Energy Electr. Eng. Symp. (AEEES), Chengdu, China, May 2020, pp. 416420.
[7] W. Wu, S. Xie, Z. Zhang, and J. Xu, ``Analysis and design of control strategy for MMC-BDC based ultra-capacitors energy storage systems," IEEE Trans. Power Electron., vol. 34, no. 27, pp. 45684575, Sep. 2014.
[8] K. Bi, L. Sun, Q. An, J. Duan, and Y. Gao, ``Distributed energy balancing control strategy for energy storage system based on modular multilevel DCDC converter," Trans. China Electrotech. Soc., vol. 33, no. 16, pp. 38113821, Aug. 2018.
[9] N. Li, L. Zhang, S. Ma, and F. Gao, ``Control strategy for battery energy storage system based on modular multilevel converters," Autom. Electr.Power Syst., vol. 41, no. 9, pp. 144150, May 2017.
[10] Y. Guan, Y. Xie, Y. Wang, Y. Liang, and X. Wang, ``An active damping strategy for input impedance of bidirectional dual active bridge DCDC converter: Modeling, shaping, design, and experiment," IEEE Trans. Ind. Electron., vol. 68, no. 2, pp. 12631274, Feb. 2021.

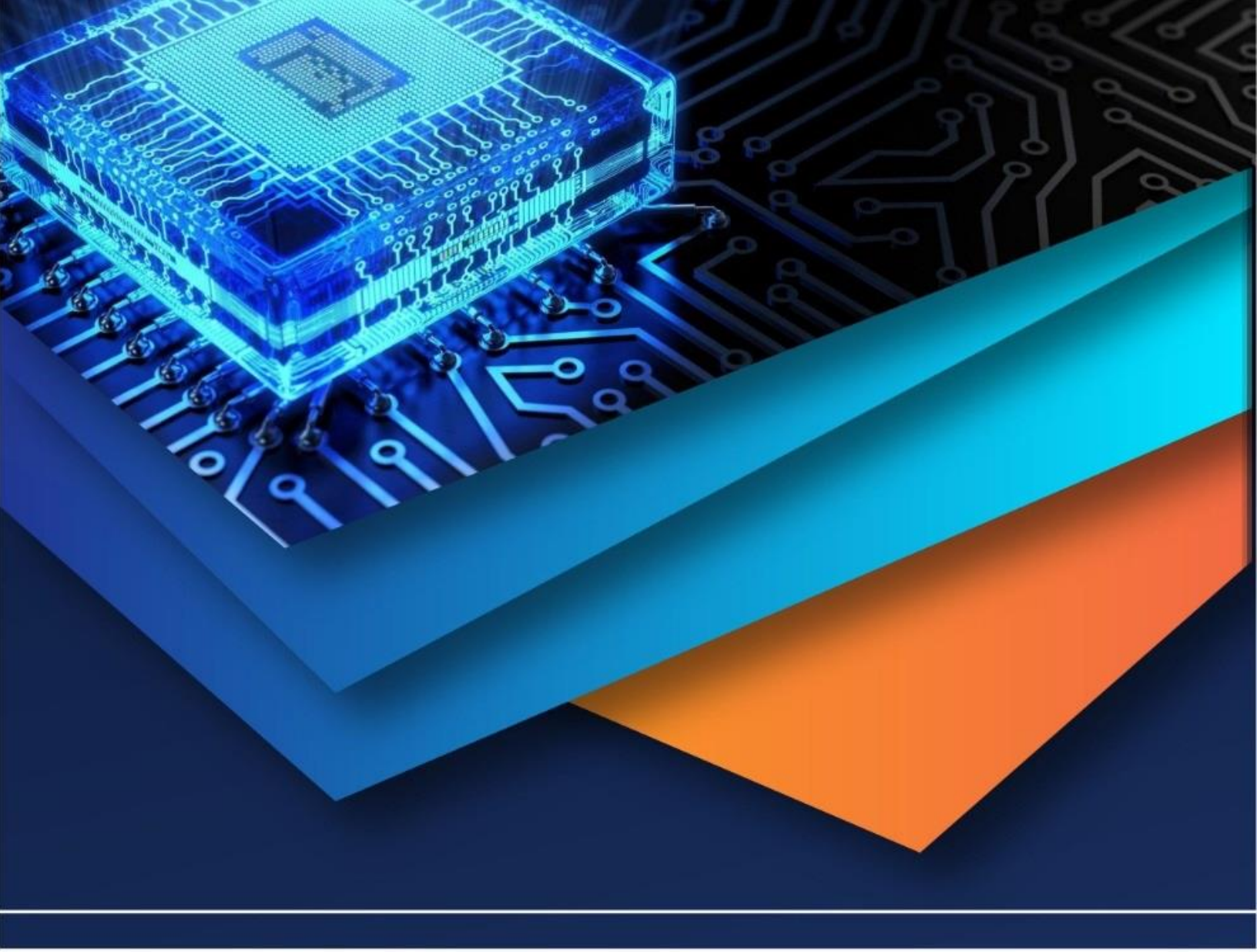

10.22214/IJRASET

45.98

IMPACT FACTOR: 7.129

IMPACT FACTOR: 7.429

INTERNATIONAL JOURNAL FOR RESEARCH

IN APPLIED SCIENCE & ENGINEERING TECHNOLOGY